01 May 2013

Aluminium-Free Glass Polyalkenoate Cements: Ion Release and in Vitro Antibacterial Efficacy

A. W. Wren

J. P. Hansen

S. Hayakawa

Mark R. Towler
Missouri University of Science and Technology, mtowler@mst.edu

Recommended Citation

A. W. Wren et al., "Aluminium-Free Glass Polyalkenoate Cements: Ion Release and in Vitro Antibacterial Efficacy," *Journal of Materials Science: Materials in Medicine*, vol. 24, no. 5, pp. 1167 - 1178, Springer, May 2013.
The definitive version is available at https://doi.org/10.1007/s10856-013-4880-y

J Mater Sci: Mater Med (2013) 24:1167–1178
DOI 10.1007/s10856-013-4880-y

Aluminium-free glass polyalkenoate cements: ion release and in vitro antibacterial efficacy

A. W. Wren · J. P. Hansen · S. Hayakawa · M. R. Towler

Received: 10 December 2012 / Accepted: 25 January 2013 / Published online: 6 February 2013

Abstract Glass polyalkenoate cements (GPCs) have exhibited potential as bone cements. This study investigates the effect of substituting TiO_2 for SiO_2 in the glass phase and the subsequent effect on cement rheology, mechanical properties, ion release and antibacterial properties. Glass characterization revealed a reduction in glass transition temperature (T_g) from 685 to 669 °C with the addition of 6 mol % TiO_2 (*AT-2*). Magic angle spinning nuclear magnetic resonance (MAS-NMR) revealed a shift from −81 ppm to −76pmm when comparing a *Control* glass to *AT-2*, indicating de-polymerization of the Si network. The incorporation of TiO_2 also increased the working time (T_w) from 19 to 61 s and setting time (T_s) from 70 to 427 s. The maximum compressive strength (σ_c) increased from 64 to 85 MPa. Ion release studies determined that the addition of Ti to the glass reduced the release of zinc, calcium and strontium ions, with low concentrations of titanium being released. Antibacterial testing in *E. coli* resulted in greater bactericidal effects when tested in aqueous broth for both titanium containing cements.

A. W. Wren (✉) · J. P. Hansen
Inamori School of Engineering, Alfred University, Alfred, NY 14802, USA
e-mail: wren@alfred.edu

S. Hayakawa
Biomaterials Laboratory, Graduate School of Natural Science and Technology, Okayama University, Okayama, Japan

M. R. Towler
Department of Biomedical Engineering, University of Malaya, Kuala Lumpur, Malaysia

M. R. Towler
Department of Mechanical and Industrial Engineering, Ryerson University, Toronto, ON, Canada

1 Introduction

Glass polyalkenoate cements (GPCs) are used as luting cements and color matched alternatives to amalgam in dentistry however their properties have potential in orthopedics. These materials typically compose of a glass phase, and acid phase (typically polyacrylic acid—PAA) and water [1]. When the components are mixed together an acid/base setting reaction occurs where the H^+ ion are liberated from the COO^- groups on the PAA chains. These ions degrade the surface of the glass particles causing partial dissolution of the glass, resulting in the release of cations (Na^+, Ca^{2+}, Al^{3+}) into the surrounding environment [1–3]. These ions crosslink the COO^- groups on the polyacid chain resulting in a set cement. These cements are known to provide therapeutic effect in vivo due to the release of ions when in an aqueous environment particularly in dental applications where the release of F^- is known to prevent the growth of secondary caries [4, 5]. However, the transition of GPCs into orthopedics has been restricted, in part, due to the release of aluminium (Al^{3+}) in the glass phase of all commercial dental materials and the subsequent release of Al^{3+} into the surrounding environment. Previous studies report the neurotoxic effects of Al^{3+} when released in body fluids, and its implication in neurological disorders such as Alzheimers and Parkinsons disease [6–8]. However the composition of the glass phase can be modified in order to include ions that are reported to have a positive therapeutic effect in the body (Ca^{2+}, Sr^{2+}, Zn^{2+}) [9]. Additional attributes to using GPCs in medicine include a lack of any significant exotherm or volumetric

shrinkage upon setting [10], rheological and mechanical properties that can be tailored by modifying the composition of the glass, molecular weight and concentration of polyacrylic acid [2, 11].

Ti is regarded as being a bioactive metal and it has been employed in many areas including prosthetics in orthopedics, craniofacial and ossicular implants, as a close bone-implant interface is evident [12, 13]. Ti has been used as coatings on implants, Ti–N coatings [14], and it has also been incorporated in bioactive glasses [15–18] and gels [19] which have reported positive surface precipitation reactions when tested in simulated body fluid [20–23]. Ti(IV) compounds can be incorporated into the GPC glass phase as where it can act as a network intermediate. In the glass phase of traditional GPCs, Al^{3+} acts as a network intermediate, predominantly as a network former, until a threshold is reached where a Si:Al ratio of >1 exists, in this instance the Al^{3+} adopts a six fold coordination state and acts as a network modifier [24]. Ti incorporation into bioactive glass has previously been investigated by the authors using X-ray photoelectron spectroscopy (XPS) and Raman spectroscopy, which determined that Ti incorporation into similar glasses acts predominantly as a network modifier [25]. This suggests that the incorporation of Ti into the glass phase results in greater dissolution when immersed in an aqueous environment. This is achieved by Ti breaking the Si–O–Si bonds, thereby increasing the concentration of non-bridging oxygens (NBO) in the glass [17]. By increasing the concentration of NBOs in the glass, ion exchange between the glass surface and an aqueous medium can be facilitated which is considered an important characteristic in bioactive materials [26].

Additional components of the glass phase include strontium, which is currently used to treat metabolic bone diseases such as osteoporosis as it increases the proliferation of osteoblasts and inhibits the action of osteoclasts in vivo [27, 28]. Zinc is also contained in the glass as it has antibacterial properties[29, 30] and has also been identified as having positive effects regarding bone turnover [31, 32]. This study was undertaken to investigate the effect of incorporating titanium (Ti) into the glass phase of a GPC series and to relate its structural effect to ion release and antibacterial properties.

2 Materials and methods

2.1 Glass synthesis

Three glasses were formulated for this study. The Si content of the glass was substituted by Ti throughout the series, *AT-1* and *AT-2* (Table 1). A Ti-free glass (*Control*) was used as a control glass for comparison. Glasses were prepared by weighing out appropriate amounts of analytical grade reagents and ball milling (1 h). The powdered mixes were oven dried (100 °C, 1 h) and fired (1,500 °C, 1 h) in platinum crucibles and shock quenched in water. The resulting frits were dried, ground and sieved to retrieve glass powders with a maximum particle size of 45 μm.

Table 1 Glass formulations (mol. Fr.)

	Control	*AT-1*	*AT-2*
SiO_2	0.48	0.45	0.42
TiO_2	0.00	0.03	0.06
ZnO	0.36	0.36	0.36
CaO	0.12	0.12	0.12
SrO	0.04	0.04	0.04

2.2 Glass characterisation

2.2.1 X-ray diffraction (XRD)

Diffraction patterns were collected using a Siemens D5000 X-ray Diffraction Unit (Bruker AXS Inc., WI, USA). Glass powder samples were packed into standard stainless steel sample holders. A generator voltage of 40 kV and a tube current of 30 mA was employed. Diffractograms were collected in the range $10° < 2\theta < 80°$, at a scan step size 0.02° and a step time of 10 s.

2.2.2 Network connectivity(NC)

The network connectivity of the glasses was calculated with Eq. 1 using the molar compositions of the glass. Network connectivity calculations were performed assuming that Ti performs as a network former and also as a network modifier

$$NC = \frac{No.BOs - No.NBOs}{Total\ No.\ Bridging\ Species} \quad (1)$$

where NC is the network connectivity, BO is the bridging oxygens, NBO is the non-bridging oxygens

2.2.3 Differential thermal analysis (DTA)

A differential thermal calorimetry analyzer (DSC, Q10-DSC, TA Instrumental Inc., New Castle, DE) was used to measure the glass transition temperature (T_g) for each glass. A heating rate of 20 °C/min was used in a nitrogen atmosphere up to a maximum temperature of 1,300 °C, using an alumina reference in a matched platinum crucible.

2.2.4 Particle size analysis (PSA)

Particle size analysis was achieved using a Beckman Coulter Multisizer 4 Particle size analyzer (Beckman

Coulter, Fullerton, CA, USA). The glass powder samples were evaluated in the range of 0.4–100.0 μm and the run length took 60 s. The fluid used in this case was water and was used at a temperature range of between 10 and 37 °C. The relevant volume statistics were calculated on each glass.

2.2.5 X-Ray photoelectron spectroscopy

XPS was performed using a PHI Quantera SXM Scanning X-ray Microprobe to determine the composition of each material. The Analytical parameters include a 100 μm spot size, 25 W, 15 kV, 240 eV pass energy, 0.5 eV step size, 3 sweeps, and a binding energy range of 0–1,100 eV. Spot size, power, and voltage were held consistent, however the pass energy and step size was reduced to 55 and 0.05 eV respectively, and the number of sweeps was raised to 5.

2.2.6 Magic angle spinning–nuclear magnetic resonance (MAS–NMR)

^{29}Si MAS NMR spectra were recorded at 7.05 T (tesla) on a Varian $^{\text{UNITY}}$INOVA300 FT-NMR spectrometer (Palo Alto, CA, USA), equipped with a CP-MAS probe. The glass samples were placed in a zirconia sample tube with a diameter of 7 mm. The sample spinning speed at the magic angle to the external magnetic field was 5 kHz. ^{29}Si MAS NMR spectra were taken at 59.59 MHz with 7.0-μs pulse length (pulse angle, π/2), 100-second recycle delays, where the signals from 2126, 1837 and 1880 pulses were accumulated for *Control*, *AT-1* and *AT-2*, respectively. ^{29}Si NMR chemical shifts are reported in ppm, with PDMS (polydimethyl silane) as the external reference (−34 ppm vs. TMS 0 ppm). All NMR spectra were recorded in a room for exclusive use of NMR, where the room temperature was kept at 300° K by means of an air-conditioner.

2.3 Handling and mechanical properties

2.3.1 Cement preparation

Cements were prepared by thoroughly mixing the glass powders (<45 μm) with polyacrylic acid (PAA—M*w*, 210,000, <90 μm, Advanced Healthcare Limited, Kent, UK) and distilled water on a glass plate. The cements were formulated with a powder to liquid (P:L) ratio of 2:1.5 with 50, 55 and 60 wt% additions of PAA. Complete mixing was undertaken within 20 s.

2.3.2 Working and setting times

The setting times (T_s) of the cement series were tested in accordance with ISO9917 [33] which specifies the standard for dental water based cements. T_s was measured by lowering a 400 g mass attached to a Gilmore needle into a cement filed mould measuring 8 × 10 mm internal diameter. Cements were stored at 37 °C during setting and the T_s was taken as the time the needle failed to make a complete indent in the cement surface, (where $n = 3$). The working time (T_w) of the cements was measured under standard laboratory conditions (Ambient Temp, $A_T \sim 25$ °C), and was defined as the period of time from the start of mixing during which it was possible to manipulate the material without having an adverse effect on its properties. Each sample (where $n = 3$), was measured using a stopwatch on a clean glass plate with a sterile spatula. Each measurement was conducted under the same mixing conditions to ensure reproducibility.

2.3.3 Compressive strength

The compressive strengths (σ_c) of the cements (6 × 4 ϕ mm, where $n = 5$) were evaluated in accordance with ISO9917 [33]. Cylindrical samples were tested after 1, 7 and 30 days. Samples were stored in sterile de-ionized water in an incubator at 37 °C. At each time period the cements were removed and tested while wet on an Instron 4082 Universal Testing Machine (Instron Ltd., High Wycombe, Bucks, UK) using a 5 kN load cell at a crosshead speed of 1 mm/min. The σ_c was calculated using Eq. 2.

$$C = \frac{4\rho}{\pi d^2} \tag{2}$$

where ρ is the maximum applied load (N), d is the diameter of sample (mm)

2.4 Ion release studies

Each cement formulation, *Control*, *AT-1* and *AT-2* (6 × 4 ϕmm, where $n = 3$) was exposed to sterile de-ionised H_2O for 1, 7 and 30 days. Cement cylinders were submerged in 10 ml of de-ionised H_2O and rotated on an oscillating platform at 37 °C. The ion release profile of each cement was measured using Inductively Coupled Plasma–Optical Emission Spectroscopy (ICP–OES) on a Perkin-Elmer Optima 3000DV (Perkin Elmer, MA, USA). ICP–OES calibration standards for Ti, Ca, Zn and Sr ions were prepared from a stock solution on a gravimetric basis. Three target calibration standards were prepared for each ion and de-ionized water was used as a control.

2.5 Antibacterial analysis

2.5.1 Bacterial broth analysis

Cement samples (6 × 4 ϕmm, where $n = 3$) were immersed in 1 ml cuvettes of bacterial broth (10 μl of 1/50 dilution, or

$\sim$1/100 dilution per 1 ml) containing *E. coli* over a time period of 0, 12, 36, 60, 84, 108 h in a sterile incubator at 37 °C. At each time period the broth was examined by UV–Visible light spectroscopy (Pharmacia biotech ultrospec 3000UV/Visible light spectrophotometer) for the % transmission (%T) through the liquid medium. The cement samples (*Control*, *AT-1* and *AT-2*) were compared against a growing population of *E. coli* at each time period. A sterile control (with sterile de-ionized H_2O used for 1/100 dilution) was also analyzed at each time period which had a %T of $\sim$92 %.

2.5.2 Agar disc-diffusion test

The antibacterial activity of the cements (6×4 ϕmm, where $n = 3$) were evaluated using *E. coli* strain ATCC 8739, using the agar diffusion method. Each cement sample (*Control*, *AT-1* and *AT-2*) were placed in inoculated plates and the plates were cultured for 24 h at 37 °C. Cement samples from ICP solutions were used to obtain data with respect to maturation (1, 7, 30 days). Luria agar and broth were used for the culture of *E. coli*, which was grown aerobically at 37 °C. Preparation of the agar disc-diffusion plates involved seeding agar plates with a sterile swab dipped in a 1/50 dilution of the appropriate 16 h culture of bacteria. The agar diffusion test was performed under standard laboratory sterile conditions in a fumigation hood using sterile swabs for inoculation of bacteria. Calipers were used to measure zones of inhibition where each sample was analyzed in triplicate and mean zone sizes $\pm$ standard deviations were calculated. Inhibition zone sizes were calculated using Eq. 3

$$Inhibition\ Zone(mm) = \frac{Halo\phi - Disc\phi}{2} \quad (3)$$

2.6 Statistical analysis

One-way analysis of variance (ANOVA) was employed to compare the antibacterial efficacy of the experimental materials considering the broth dilution test specifically considering (1) immersion time and (2) comparison of experimental materials (*Control*, *AT-1*, *AT-2*) with a growing bacterial culture. Inhibition zone measurements were also analyzed from the agar-diffusion test. Comparison of relevant means was performed using the post hoc Bonferroni test. Differences between groups was deemed significant when $p \leq 0.05$.

3 Results and discussion

3.1 Glass characterization

The objective of this work is to relate the structure of the glass, in particular the role of Ti, when substituted in a SiO_2–ZnO–CaO–SrO series of bioactive glass, to ion release and antibacterial efficiency. Initial characterization included x-ray diffraction (XRD), network connectivity calculations (NC) and particle size analysis (PSA). Figure 1a shows the XRD patterns of each glass, *Control*, *AT-1* and *AT-2*, and confirms that each starting material was amorphous. Figure 1b shows the NC calculations based on the assumption that Ti acts as both a network former and a network modifier. Assuming that Ti acts as a network former the NC will not change from 1.83 as the Si concentration is being substituted by the Ti. However, if it is assumed that the Ti acts as a network modifier, the NC decreases from 1.83 (*Control*), to 1.56 (*AT-1*) to 1.24 (*AT-2*). This reduction in NC arises from a higher concentration of network modifier ions, and is related to the concentration of non-bridging oxygen (NBO) within the glass network. Figure 1c shows the PSA of each of the glass particles, and determined that each glass had a similar size which ranged between 4.2 and 4.9 μm.

XPS was employed in order to confirm the presence of each of the elements incorporated into the individual glasses. Figure 2 shows the survey scans of two representative glasses, the *Control* glass and *AT-2*. The control glass was found to contain, Zn, O, Ca, Sr and Si, while both *AT-1* and *AT-2* contain each of these elements in addition to Ti. The Ti at this binding energy (458 eV) is associated with TiO_2. Additionally, carbon was also detected which is likely due to sample preparation.

A thermal profile of each of the glasses was achieved using differential thermal analysis (DTA) and is presented in Fig. 3. Figure 3a shows the thermal profile of the *Control* glass which has a glass transition temperature (T_g) of 685 °C, a primary crystallization peak (T_{c1}) at 848 °C, a secondary crystallization peak (T_{c2}) at 939 °C, and a melting temperature (T_m) at 1155 °C. When comparing *AT-1* (3 mol% TiO_2) to the *Control* glass, it is evident that there is a reduction in the T_g (674 °C), also T_{c1} and T_{c2} reduce to 828 and 929 °C respectively and the T_m reduced to 1,112 °C. A greater effect was found when comparing *AT-2* (6 mol% TiO_2) to the *Control* glass. Figure 3c shows the thermal profile of *AT-2* which shows a greater reduction in the T_g (669 °C), also T_{c1} and T_{c2} reduce to 821 and 903 °C and the T_m reduced to 1,103 °C. The reduction in the thermal characteristics as a result of the increasing addition of Ti may be attributed to de-polymerization of the continuity of the silicate network by breaking of the Si–O–Si bonds. This is indicative of increased network disruption which is facilitated by the incorporation of network modifiers in the glass.

Further analysis of the glass structure was completed using magic angle spinning nuclear magnetic resonance (MAS–NMR), which is an analytical tool that is widely used for investigating the structure of glass. An established

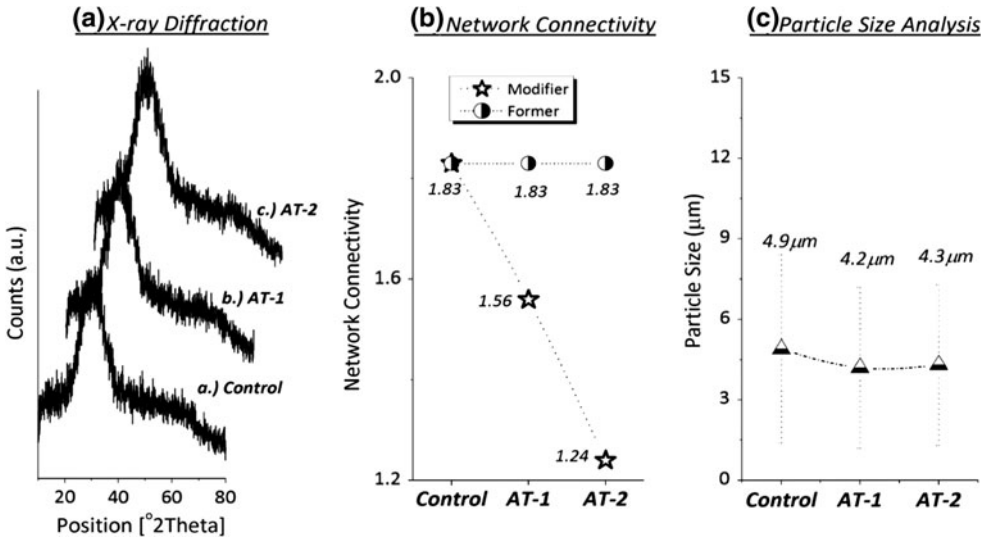

Fig. 1 **a** XRD patterns, **b** network connectivity calculations and **c** particle size analysis of glass series

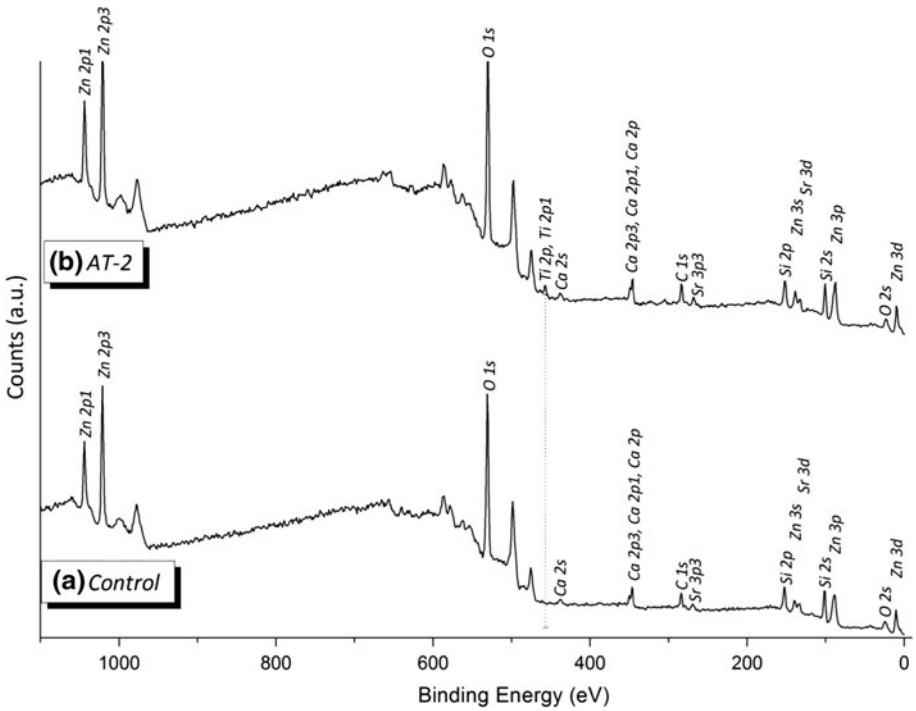

Fig. 2 XPS survey scans of **a** *Control* and **b** *AT-2*

method to represent structural arrangement within a glass can be represented by Q^n units, where Q represents the Si tetrahedral unit and n the number of bridging oxygens (BO); n ranges between 0 and 4. Si is the central tetrahedral atom which ranges from Q^0 (orthosilicates) to Q^4 (tectosilicates) and Q^1, Q^2 and Q^3 structures represent intermediate silicates containing modifying oxides that depolymerize the silicate network [34]. Si^{29} MAS-NMR was performed in order to probe the local environment of the Si atom. Figure 4 shows the MAS–NMR spectra of the *Control*, *AT-1* and *AT-2*. The *Control* spectra, presented in Fig. 4, was found to have a peak position of −81 ppm, while *AT-1* and *AT-2* had chemical shifts in the positive direction to −77 and −76 ppm respectively. A shift in ppm in a positive direction, as presented with *AT-1* and *AT-2*, is indicative of an increase in NBO species within the glass. Previous studies have identified regions where the chemical shift represents structural changes around the Si atom which lie in the region of −60 to −120 ppm for SiO_4 tetrahedra [35]. Previous NMR studies by Galliano et al. and Hayakawa et al. [36, 37] on silicate melts suggest the presence of Q^1, Q^2 and Q^3 species at −78, −85 and −95 ppm respectively. This suggests that the *Control* glass contains both Q^1/Q^2, *AT-1* and *AT-2* can be described as being predominantly Q^1. However, the broadness of the spectral envelope in each case suggests the presence of multiple Q-species.

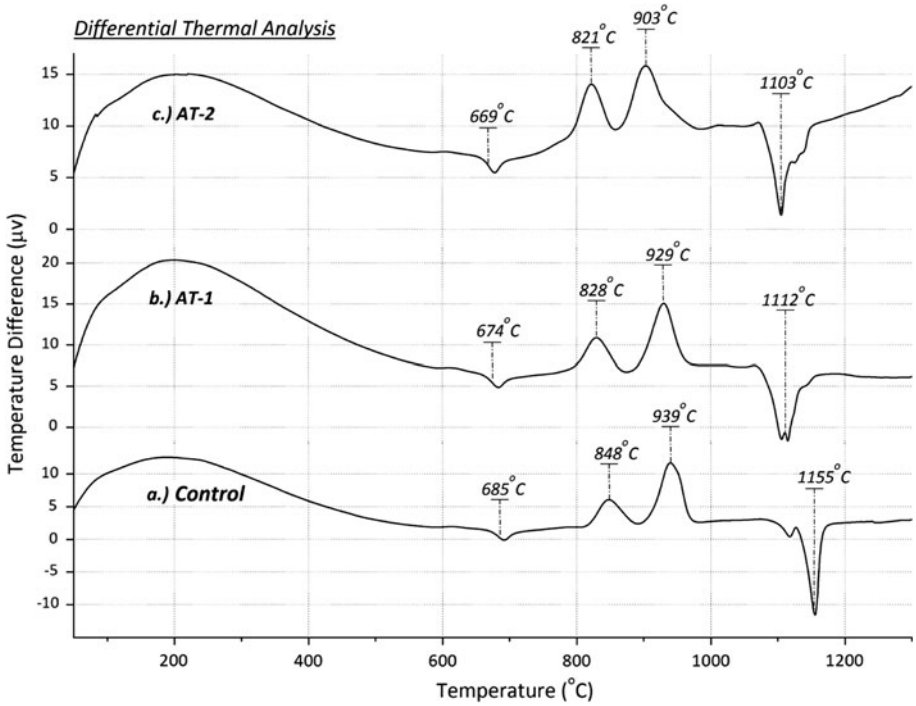

Fig. 3 Thermal profile of each glass determined by DTA

Deconvolution of each spectrum supports the evidence of increasing NBO content with increasing TiO_2 concentration in the glass. In Fig. 4 the larger band is present at −80 ppm in the *Control,* while the same band is present at −77 ppm for both *AT-1* and *AT-2*. The smaller asymmetric shoulders were determined to be present at −88 ppm (*Control*), −85 ppm (*AT-1*) and −83 ppm (*AT-2*), which supports the hypothesis that Ti acts as a network modifier in the glass encouraging the formation of Si–O–NBO species. This correlates with the network connectivity predictions when Ti is assumed to be a network modifier and also the changes presented with the reduction in T_g associated with the increase in TiO_2 concentration.

3.2 Handling and mechanical properties

The T_w and T_s of the cement series was evaluated with respect to two parameters, the increasing concentration of TiO_2 in the glass phase and also the concentration of PAA used. The T_w are presented in Fig. 5a and shows a similar trend with each material where the increase in PAA concentration results in a decreased T_w. This is as expected and is due to the higher concentration of COO^- groups available for binding of metal cations. The *Control* exhibited T_w of 19 s (50 wt%), 11 s (55 wt%) and 9 s (60 wt%) respectively, which are too short for any clinical application. *AT-1* exhibited T_w of 25 s (50 wt%), 22 s (55 wt%),

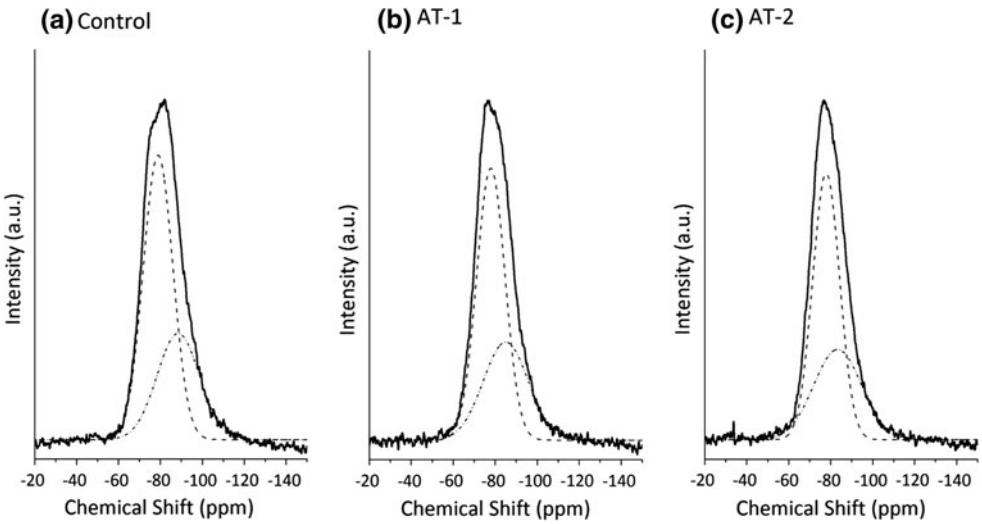

Fig. 4 MAS–NMR of **a** *Control*, **b** *AT-1* and **c** *AT-2*

and 18 s (60 wt%) and *AT-2,* 61 s (50 wt%), 42 s (55 wt%) and 35 s (60 wt%) respectively. The T_s are presented in Fig. 5b and exhibited a similar trend to the T_w where the increase in PAA concentration results in a reduction in T_s. The *Control* material presented T_s of 70 s (50 wt%), 55 s (55 wt%) and 51 s (60 wt%) respectively. *AT-1* exhibited longer T_s than the *Control* and were determined to be 95 s (50 wt%), 83 s (55 wt%) and 75 s (60 wt%), while *AT-2* exhibited longer T_s than both *Control* and *AT-1* at 427 s (50 wt%), 415 s (55 wt%) and 385 s (60 wt%) respectively. The setting characteristics associated with *AT-2* are preferable when compared to the *Control* and *AT-1*, as clinically relevant materials are expected to have a T_s of $\sim$5 min (300 s) [38]. *AT-1* exhibited T_s of 7:06 min (427 s), 6:54 min (415 s), 6:36 min (385 s) respectively by modifying the concentration of PAA.

Mechanical testing (σ_c) was undertaken in order to determine with formulation produced the highest strength. The compression testing was conducted with respect to TiO_2 concentration in the glass and also PAA concentration. An additional parameter was investigated also, the effect of maturation time. Regarding the *Control* cement, the σ_c was observed to increase with respect to both TiO_2 concentration in the glass, and also PAA concentration. The *Control* cement produced maximum strengths of 65 MPa with 60 wt% PAA after 7 days and reduced to 42 MPa after 30 days. A similar trend was observed with *AT-1* where the maximum strength was 82 MPa with 60 wt% PAA after 7 days and reduced to 54 MPa after 30 days. This may be attributed to water absorption resulting in plasticizing effects, however previous studies by Nicholson and Abiden [39] demonstrate that GPCs formed from acrylic-maleic acid copolymers reduce in compressive strength in media other than water, suggesting that an additional time-dependant factor results in the reduction is strength, such as an increase in brittleness as cross-linking continues. Further mechanical testing, such as fracture toughness, would be required to further explore this phenomenon. *AT-2* was found to have a highest compressive strength of 85 MPa with 55 wt% PAA after 7 days. A reduction in compressive strength after 30 days was also observed, however it was not found to be significantly reduced. These results suggest that the addition of Ti to the glass phase, and the higher concentration of PAA results in cements with higher mechanical properties, however, the compressive strengths are still significantly lower than the commercially available materials, which is likely due to differences in glass composition, the acid components used (PAA and PAA copolymers) and the specific formulation used Fig. 6.

This increase in compressive strength of these GPCs can primarily be attributed to the incorporation of Ti into the glass phase. The addition of Ti increases the T_w and T_s which facilitates greater chelation between the COO^- groups (particularly at higher PAA concentrations, 55, 60 wt%) and metal cations released into the cement polysalt matrix.

3.3 Ion release studies

Ion release studies were undertaken in order to evaluate the solubility of the cements in relation to Ti incorporation into

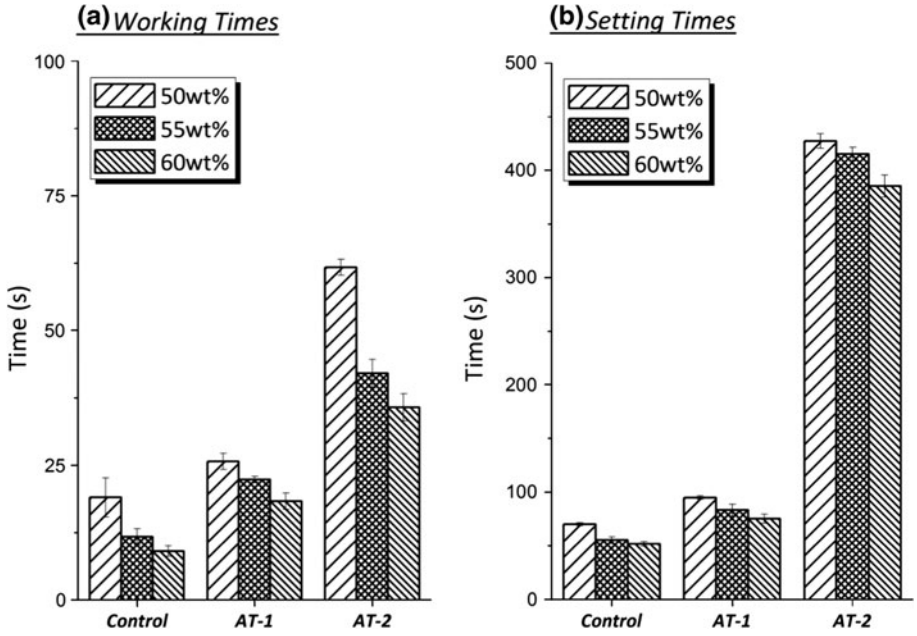

Fig. 5 **a** Working times and **b** setting times of cement series

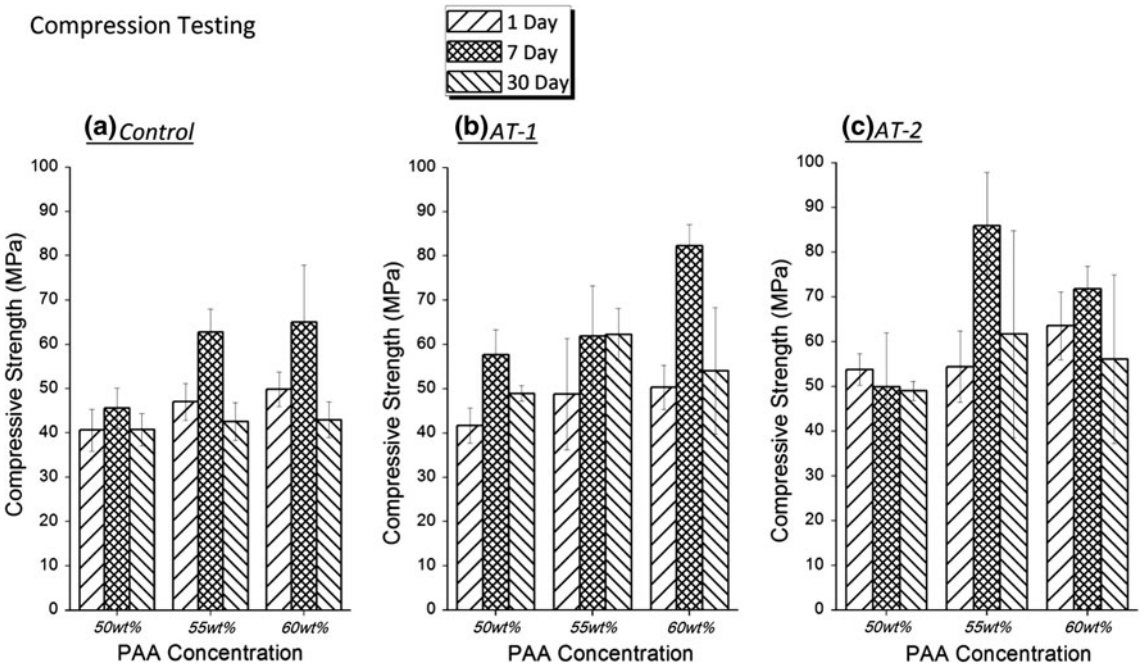

Fig. 6 Compressive strength of E11 cements over 1–30 days

the glass phase. In general ion release from each cement was low, which may be due in part to the concentration (50 wt%) and molecular weight of the acid used. For the ion release studies 50 wt% PAA was selected as it demonstrates superior rheological properties, and also this formulation will likely yield higher ion release values than 55 or 60 wt% PAA additions. The ion release profiles are presented in Fig. 7. Figure 7a shows the release of zinc (Zn) over 1, 7 and 30 days. Zn release was found to increase over 1, 7 and 30 days, which had a maximum of 3.0 μg/L. Interestingly, the addition of Ti to the glass phase resulted in a reduction of Zn release to ~1.2–1.4 μg/L. Figure 7b shows the calcium (Ca) release which also showed an increase in ion release over 1, 7 and 30 days. Ca release peaked at 4.5 μg/L after 30 days. Similarly to Zn, the addition of Ti to the glass phase resulted in a reduction in Ca release, which seems to be directly related to Ti concentration, *AT-1* (1.9 μg/L) and *AT-2* (1.2 μg/L). Figure 7c shows the strontium (Sr) release from the cements. Sr was observed to also increase in the *Control* cement with increasing exposure time with a maximum of 5.6 μg/L after 30 days. Similar to both Zn and Ca, Sr ion release was found to decrease with the addition of Ti in the glass phase. This was also a function of Ti concentration where Sr levels reduced to 2.0 and 1.27 μg/L in *AT-1* and *AT-2* respectively. Figure 7d shows the Ti release profile from the cement series. No Ti was present in the *Control*, however very low concentrations of Ti were detected in *AT-1* (0.03 μg/L) and *AT-2* (0.02 μg/L).

One theory that may explain the reduction in ion release levels with the addition of Ti in the glass is that the incorporation of Ti in the glass phase facilitates longer *Ts*. When the cements are permitted time to mature and strengthen, the Ca^{2+}, Sr^{2+} and Zn^{2+} form crosslinks with COO^{-} groups on the PAA chains. This increase in T_s facilitates greater interconnectivity within the cement matrix resulting in an overall increase in mechanical strength and a reduction in the concentrations of released ions. Regarding the *Control* cement, the setting is too rapid to fully establish a crosslinked network and unreacted residual glass particles are degrading over time facilitating greater ion release. It may also be possible that the addition of Ti into the glass network results in depolymerising the silicate network (as observed by MAS–NMR), and during cement gelation, there is a change in the pH of the setting polysalt matrix which significantly alters the setting characteristics of the materials, resulting in a more mature, crosslinked cement matrix with the majority of the available ions contributing to mechanical strength as opposed to ion release.

3.4 Antibacterial testing

The antibacterial properties of the materials were determined using two separate tests, the broth dilution test and also the agar diffusion test. The results of the broth dilution test are presented in Fig. 8. Each solution was probed with UV/Visible light spectroscopy immediately after inoculation and

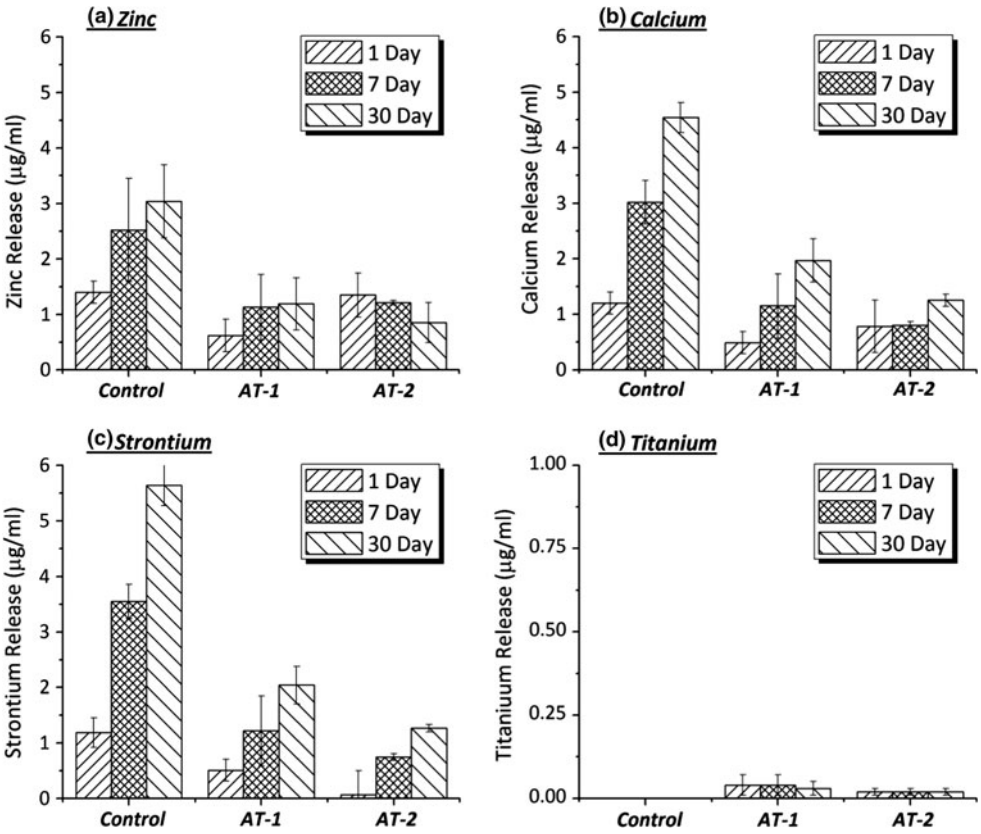

Fig. 7 Ion release profiles for Ti-cements observing **a** zinc, **b** calcium, **c** strontium and **d** titanium

obtained %T values similar to the control broth of ~92 %. As the incubation time increased the %T of the bacteria containing broth was seen to decrease to 45 % (12 h) and ranged between 28 and 32 % over 36–108 h. Statistical analysis was performed with respect to immersion time (Table 2) and it was determined that the bacterial broth showed a significant reduction in %T over 0–60 h ($P = 0.000$) which then stabilized over 60–108 h ($P = 1.000$). This was expected as the proliferation of the bacteria in the broth results in increased cell density, thereby restricting the passage of light through the medium. The *Control* cement maintained a high %T over 0–60 h where the %T ranged from 91 to 94 % (0–60 h, $P = 1.000$). After 84 h the %T reduced to 84 % and after 108 h the %T reduced further to 67 % (60–108 h, $P = 0.000$). A similar trend was also observed with the Ti containing cements where for *AT-1* and *AT-2* the %T ranged from 86 to 91 % over 0–60 h which was not deemed a significant reduction ($P = 1.000$). At 108 h the %T reduced to 69 and 76 % for *AT-1* (60–108 h, $P = 1.000$) and *AT-2* respectively (60–108 h, $P = 1.000$) which also did not exhibit a significant reduction in %T. This is a positive result as the *AT-1* and *AT-2* materials experienced less deviation from the original sterile broth than the *Control* material, suggesting that the proliferation of bacteria was greatly reduced in cultures containing *AT-1* and *AT-2*. The slight reduction in %T over time is most likely due to the

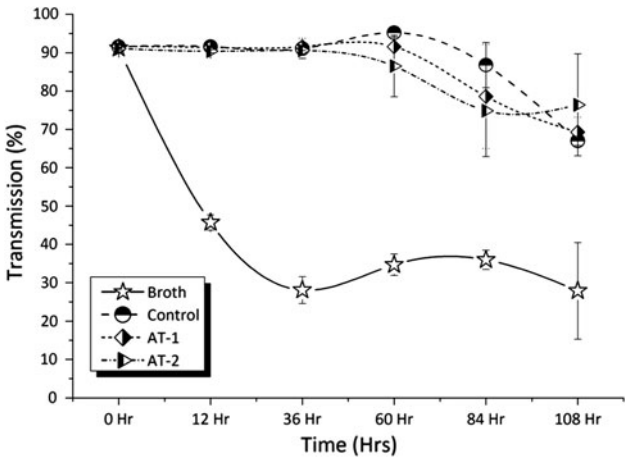

Fig. 8 Broth dilution antibacterial analysis of cements in *E. coli* broth

increase in the number of bacterial cells which were not initially eradicated as a result of either ion release from the cement, or pH changes within the bacterial broth as a result of the ion release. Statistical analysis (Table 3) was performed comparing the experimental materials to the bacterial broth and it was found the in each case the *Control*, *AT-1* and *AT-2* initially (at 0 h) there was no difference ($P = 1.000$, $P = 0.703$, $P = 1.000$ respectively), however at each time

Table 2 Means comparison of broth dilution test with respect to immersion time

	0–60 h	60–108 h
Broth	0.000*	1.000
Control	1.000	0.000*
AT-1	1.000	0.120
AT-2	1.000	1.000

* Significant at 0.05 level

Table 3 Means comparison of materials and bacterial broth at each time period

	0 h	12 h	36 h	60 h	84 h	108 h
Broth versus Control	1.000	0.000*	0.000*	0.000*	0.001*	0.005*
Broth versus AT-1	0.703	0.000*	0.000*	0.000*	0.004*	0.004*
Broth versus AT-2	1.000	0.000*	0.000*	0.000*	0.007*	0.001*

* Significant at 0.05 level

period following the initial time point, there was a significant change in %T ($P = 0.000$–0.007).

The agar diffusion test was also performed where maturation time was also considered. Cement samples were aged for 1, 7 and 30 days in sterile de-ionized water to determine if antibacterial efficacy is retained after prolonged periods of time in solution. Figure 9 shows the results of the agar diffusion test. It is evident from Fig. 9 that each cement sample exhibits a greater antibacterial effect when initially tested as opposed to being subjected to immersion in an aqueous environment over prolonged periods of time. At 0 day, the cements exhibited inhibition zones of 3.5, 3.4 and 3.3 mm for *Control*, *AT-1* and *AT-2* respectively. The inhibition zones exhibited by the *Control* (3.7 mm, $P = 1.000$) after 1 day immersion in solution were similar to 0 day samples, however *AT-1* (1.6 mm, $P = 0.000$) and *AT-2* (1.5 mm, $P = 0.000$) were found to reduce. The *Control* sample reduced at 7 days (2.2 mm) and then recovered after 30 days to 3.2 mm, which was determined as insignificant ($P = 0.000$) when compared to the initial samples (0 day). Both *AT-1* and *AT-2* did not significantly change over 1–7 and 7–30 days (Table 4), however both were found to significantly reduce over time when compared to initial sample (0 day, $P = 0.000$). This is as expected as ions leached from the cements accumulate in solution over time; however the cements retained some of their antibacterial nature even after prolonged periods of time in water. This suggests that some of the antibacterial ions are residing within the cement over long periods of time or that ion exchange is occurring between the cement and the solution in which the cements were immersed. Also when comparing the *Control* to *AT-1* ($P = 0.881$) and *AT-2* ($P = 0.238$) at 0 day it was found that there was no significant difference in inhibition zone.

Table 4 Means comparison considering antibacterial agar diffusion testing

Day	*BT 101*	*AT-1*	*AT-2*
0 versus 1	1.000	0.000*	0.000*
1 versus 7	0.000*	0.130	1.000
7 versus 30	0.004*	1.000	0.230
0 versus 30	1.000	0.000*	0.000*

* Significant at 0.05 level

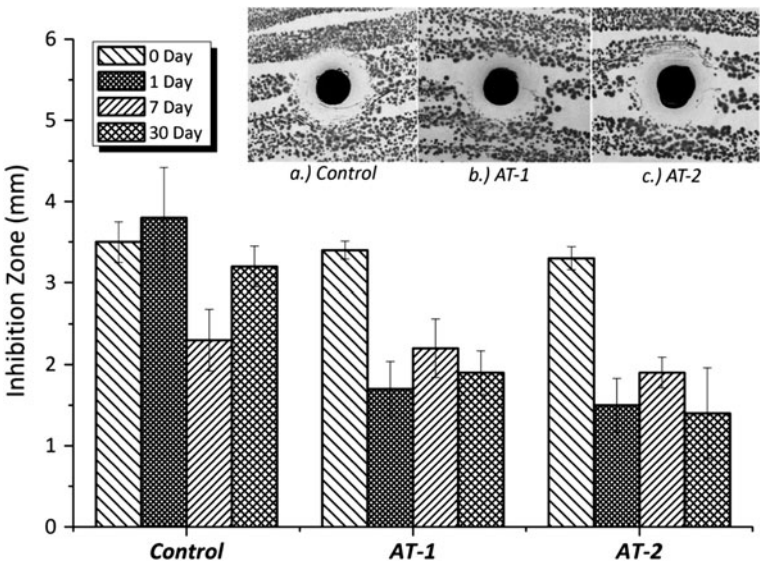

Fig. 9 Agar diffusion antibacterial analysis of cements in *E. coli* (*inset*, each cement at 0 days)

4 Conclusion

From this study it appears that the substitution of Ti into the glass for Si, results in greater depolymerisation of the silicate network by breaking the Si–O–Si bonds. This leads to greater dissolution of the glass particles when mixed with PAA and water which subsequently results in greater handling and mechanical properties when compared to the *Control*. However, the Zn, Ca and Sr ion release was found to decrease when Ti was substituted into the glass, which may be attributed to these ions contributing to the compressive strength of the cements. It was also determined that the broth dilution antibacterial testing revealed greater antibacterial properties over the *Control*, while the agar diffusion testing did not reveal any significant difference. Future work on these materials will include testing these glass compositions with different molecular weight PAA, investigating the effect on ion release and the subsequent effect in cell culture and relevant animal models.

References

1. Nicholson JW. Chemistry of glass ionomer cements. Biomaterials. 1998;19:485–94.
2. Nicholson JW, Wilson AD. Acid-base cements: their biomedical and industrial applications. Chemistry of Solid State Materials, vol. 3. Cambridge: Cambridge University; 1993.
3. Griffin S, Hill R. Influence of poly(acrylic acid) molar mass on the fracture properties of glass polyalkenoate cements. J Mater Sci. 1998;33:5383–96.
4. Vermeersch G, Leloup G, Vreven J. Fluoride release from glass–ionomer cements, compomers and resin composites. J Oral Rehabil. 2001;28:26–32.
5. Marczuk-Kolada G, Jakoniuk P, Mystkowska J, Luczaj-Cepowicz E, Waszkiel D, Dabrowski JR, Leszczynska K. Fluoride release and antibacterial activity of selected dental materials. Postepy Higieny Medycyny Doswiadczalnej. 2006;60:416–20.
6. Hoang-Xuan K, Perrotte P, Dubas F, Philippon J, Poisson FM. Myoclonic encephalopathy after exposure to aluminium. The Lancet. 1996;347:910–11.
7. Polizzi S, Pira E, Ferrara M, Bugiani M, Papaleo A, Albera R, Palmi S. Neurotoxic effects of aluminium among foundry workers and Alzheimers disease. Neurotoxicity. 2002;23:761–74.
8. Reusche E, Pilz P, Oberascher G, Linder B, Egensperger R, Gloeckner K, Trinka E, Iglseder B. Subacute fatal aluminium encephalopathy after reconstructive otoneurosurgery: a case report. Hum Pathol. 2001;32(10):1136–9.
9. Carter DH, Sloan P, Brook IM, Hatton PV. Role of exchanged ions in the integration of ionomeric (glass polyalkenoate) bone substitutes. Biomaterials. 1997;18:459–66.
10. Boyd D, Towler MR, Wren AW, Clarkin OM, Tanner DA. TEM analysis of apatite surface layers observed on zinc based glass polyalkenoate cements. J Mater Sci. 2008;43:1170–3.
11. Wilson AD, McLean JW. Glass-ionomer cement. Chicago: Quintessence Publishing Company; 1988.
12. Schwager K. Titanium as a biomaterial for ossicular replacement: results after implantation in the middle ear of the rabbit. Eur Arch Otorhinolaryngol. 1998;255:396–401.
13. Lausmaa J. Surface spectroscopic characterization of titanium implant materials. J Electron Spectrosc Relat Phenom. 1996;81:343–61.
14. Piscanec S, Ciacchi LC, Vesselli E, Comelli G, Sbaizero O, Meriani S, De Vita A. Bioactivity of TiN-coated titanium implants. Acta Mater. 2004;52:1237–45.
15. Kashif I, Soliman AA, Farouk H, Sanad AM. Effect of titanium addition on crystallization kinetics of lithium borosilicate glass. J Alloys Compd. 2009;475:712–7.
16. Satyanarayana T, Kityk IV, Ozga K, Piasecki M, Bragiel P, Brik MG, Ravi Kumar V, Reshak AH, Veeraiah N. Role of titanium valence states in optical and electronic features of PbO-Sb2O3-B2O3:TiO2 glass alloys. J Alloys Compd. 2009;482(1-2):283–97.
17. Yamanaka H, Nakahata K, Terai R. Structure of Na_2O-TiO_2-SiO_2 glasses from the viewpoint of non-bridging oxygens measured by XPS. J Non Cryst Solids 1987;95 & 96:405–410.
18. Iwamoto N, Tsunawaki Y, Masao F, Hatfori T. Raman spectra of K_2O–SiO_2 and K_2O–SiO_2–TiO_2 glasses. J Non Cryst Solids. 1975;18:303–6.
19. Kokubo T, Takadama H. How useful is SBF in predicting in vivo bone bioactivity. Biomaterials. 2006;27:2907–15.
20. Serro AP, Fernandes AC, Saramago B, Lima J, Barbosa MA. Apatite deposition on titanium surfaces—the role of albumin adsorption. Biomaterials. 1997;18:963–8.
21. Sul Y-T, Johansson C, Byon E, Albrektsson T. The bone response of oxidized bioactive and non-bioactive titanium implants. Biomaterials. 2005;26:6720–30.
22. Takadama H, Kim H-M, Kokubo T, Nakamura T. XPS study of the process of apatite formation on bioactive Ti–6Al–4V alloy in simulated body fluid. Sci Technol Adv Mater. 2001;2:389–96.
23. Byon E, Moon S, Cho S-B, Jeong C-Y, Jeong Y, Sul Y-T. Electrochemical property and apatite formation of metal ion implanted titanium for medical implants. Surf Coat Technol. 2005;200(1–4):1018–21.
24. Mysen BO, Virgo D, Kushiro I. The structural role of aluminium in silicate melts—a Raman spectroscopic study at 1 atmosphere. Am Mineral. 1981;66:678–701.
25. Wren AW, Laffir FR, Kidari A, Towler MR. The structural role of titanium in Ca–Sr–Zn–Si/Ti glasses for medical applications. J Non Cryst Solids. 2010;357(3):1021–6.
26. Serra J, Gonzalez P, Liste S, Chiussi S, Leon B, Perez-amor M, Ylanen HO, Hupa M. Influence of the non-bridging oxygen groups on the bioactivity of silicate glasses. J Mater Sci Mater Med. 2002;13:1221–5.
27. Marie PJ. Strontium ranelate: new insights into its dual mode of action? Bone. 2007;40(1):S5–8.
28. Marie PJ. Strontium ranelate; a novel mode of action optimizing bone formation and resorption. Osteoporos Int. 2005;16:S7–10.
29. Boyd D, Li H, Tanner DA, Towler MR, Wall JG. The antibacterial effects of zinc ion migration from zinc-based glass polyalkenoate cements. J Mater Sci Mater Med. 2006;17:489–94.
30. Yamamoto O. Influence of particle size on the antibacterial activity of zinc oxide International. J Inorg Mater. 2001;3:643–6.
31. King JC. Does poor zinc nutriture retard skeletal growth and mineralization in adolescents. Am J Clin Nutr. 1996;64:375–6.
32. Yamaguchi M, Ma ZJ. Role of endogenous zinc in the enhancement of bone protein synthesis associated with bone growth of newborn rats. J Miner Metab. 2001;19:38–44.
33. International Organization for Standardization 9917. Dental Water Based Cements (E), in Case Postale 56. Switzerland: Geneva; 1991. p. CH-11211.
34. Aguiar H, Serra J, Gonzalez P, Leon B. Structural study of sol-gel silicate glasses by IR and Raman spectroscopies. J Non Cryst Solids. 2009;335:475–80.

35. Stamboulis A, Law RV, Hill RG. Characterization of commercial ionomer glasses using magic angle nuclear magnetic resonance (MAS-NMR). Biomaterials. 2004;25(17):3907–13.
36. Galliano PG, Porto JM, Spezl L, Varetti EL, Sobrados I, Sanz J. Analysis by nuclear magnetic resonance and raman spectroscopy of the structure of bioactive alkaline-earth silicophosphate glasses. Mater Res Bull. 1994;29(12):1297–306.
37. Hayakawa S, Osaka A, Nishioka H, Matsumoto S, Minura Y. Structure of lead oxyfluorosilicate glasses: X-ray photoelectron spectroscopy and nuclear magnetic resonance spectroscopy and molecular dynamics simulation. J Non Cryst Solids. 2000;272: 103–18.
38. Palussiere J, Berge J, Gangi A, Cotten A, Pasco A, Bertagnoli R, Jaksche H, Carpeggiani P, Deramond H. Clinical results of an open prospective study of a Bis-GMA composite in percutaneous vertebral augmentation. Eur Spine J. 2005;14:982–91.
39. Nicholson JW, Abiden F. Changes in compressive strength on ageing in glass polyalkenoate (glass-ionomer) cements prepared from acrylic/maleic acid copolymers. Biomaterials. 1997;18:59–62.